

**→ EO CLINIC**

**Rapid-Response Satellite Earth Observation  
Solutions for International Development Projects**

**EO Clinic project:**

# **Increasing Agro-Climatic Resilience in Nigeria**

*Work Order Report*

Support requested by:  
World Bank Group (WBG)

EOC0019\_WOR\_C\_T\_v01



Reference: EOC0001\_WOR\_v01  
Date: 2021 November 12

## TABLE OF CONTENTS

Table of Contents.....	i
About this Document .....	ii
About the EO Clinic.....	ii
Authors.....	ii
Acknowledgements.....	iii
1 Development Context and Background.....	1
1.1 Increasing agro-climatic resilience in Nigeria .....	1
1.2 Objectives .....	1
2 Proposed Work Logic For EO-Based Solutions.....	2
2.1 Data .....	2
2.2 Methodology .....	4
3 Delivered EO-Based Products and Services .....	7
3.1 Raster maps.....	7
3.2 Vector maps .....	8
3.2.1 Specifications .....	9
3.2.2 Usage, Limitations and Constraints .....	9
3.2.3 NDVI annual vegetation productivity .....	9
3.2.4 Yearly productivity change and binary desert map .....	10
3.2.5 Binary vegetation maps.....	11
3.2.6 Aggregated Analysis and residual trend.....	12
4 Evaluation and Follow-up activities.....	15
4.1 Key findings .....	15
4.2 Outlook and further studies .....	19
Appendix B: References .....	20

---

## ABOUT THIS DOCUMENT

This document is the final Work Order Report of the ESA (European Space Agency) EO Clinic project EOC0019 “Increasing Agro-Climatic Resilience in Nigeria”. This publication was prepared in the framework of the EO Clinic (Earth Observation Clinic, see below), in partnership between ESA (European Space Agency), the World Bank Group (WBG) and the team of the service provider contracted by ESA: GeoVille GmbH (Austria).

This Work Order Report (WOR) describes the context of the WBG activities on increasing agro-climatic resilience in Nigeria, the geoinformation requirements of the activities and finally, the EO products and services delivered by the EO Clinic service providers in support of those activities.

This Work Order Report (WOR) is structured as in the following:

- **Section 1** describes the context of the World Bank Group (WBG) activities on detecting desertification trends in Nigeria, as well as the project objectives.
- **Section 2** highlights the applied work logic and methodologies followed.
- **Section 3** describes the services, their specifications and outputs.
- **Section 4** presents an evaluation of the data availability and suitability in support of the EO products and services under the perspective of a potential roll-out.

## ABOUT THE EO CLINIC

The EO Clinic (Earth Observation Clinic) is an ESA (European Space Agency) initiative to create a rapid-response mechanism for small-scale and exploratory uses of satellite EO information in support of a wide range of International Development projects and activities. The EO Clinic consists of “on-call” technically pre-qualified teams of EO service suppliers and satellite remote sensing experts in ESA member states. These teams are ready to demonstrate the utility of satellite data for the development sector, using their wide range of geospatial data skills and experience with a large variety of satellite data types.

The support teams are ready to meet the short delivery timescales often required by the development sector, targeting a maximum of 3 months from request to solution.

The EO Clinic is also an opportunity to explore more innovative EO products related to developing or improving methodologies for deriving socio-economic and environmental parameters and indicators.

The EO Clinic was launched in March 2019 and is open to support requests by key development banks and agencies during the 2 years project duration.

In March 2021 the project framework has been extended again for another 2 years.

## AUTHORS

The present document was prepared and coordinated by **Norman Kießlich** (Head of International Development, GeoVille) with support from the following contributors: **Philipp Rastner** (Project Manager, GeoVille), **Stefan Ralser** (Senior EO Technician, GeoVille) and **Michael Riffler** (Head of EO Innovation, GeoVille).

---

## ACKNOWLEDGEMENTS

The following colleagues provided valuable inputs, insights and evaluation feedback on the work performed: Maurizio Guadagni (Sr. Agriculture Development Specialist, WBG) and Nagaraja Rao Harshadeep (Lead Environmental Specialist, WBG).

For further information	Please contact Philipp Rastner, Project Manager, GeoVille ( <a href="mailto:rastner@geoville.com">rastner@geoville.com</a> ) with copy to <a href="mailto:Zoltan.Bartalis@esa.int">Zoltan.Bartalis@esa.int</a> if you have questions or comments with respect to content or if you wish to obtain permission for using the material in this report.  Visit the ESA EO Clinic: <a href="https://eo4society.esa.int/eo_clinic">https://eo4society.esa.int/eo_clinic</a> .
-------------------------	---

---

# 1 DEVELOPMENT CONTEXT AND BACKGROUND

## 1.1 Increasing agro-climatic resilience in Nigeria

### Desertification in Nigeria

Nigeria encompasses various climatic regimes with tropical rain forests in the South and the Sahelian savanna in the North, which is by its nature susceptible to desertification processes. The most prominent climatic parameters influencing desertification are temperature and precipitation and both of them have already been observed to change. Temperature is anticipated to rise and the duration and the intensity of the rainfall to decrease (Ahmed *et al.*, 2020; Hoscilo *et al.*, 2015). As such, the climate of West Africa is expected to gradually become more arid (Mechiche-Alami and Abdi, 2020; IPCC, 2019). A more arid climate will facilitate desertification and as such also endanger human activities by threatening agricultural productivity and biodiversity (IPCC, 2019; Suleiman *et al.*, 2017). This poses a high risk considering that the African population and with it the demand for food is foreseen to grow faster in the future than in other regions of the world (Sedano *et al.*, 2019).

Based on these insights and knowledge gaps, the World Bank (WB) together with the Government of Nigeria are seeking satellite EO support to assess the current level of land degradation and water scarcity in the country. The aim is, after the outcomes of this EOclinic project, to better understand the extent and severity of land degradation and desertification in Nigeria in order to increase the adoption of climate resilient landscape management. This current situation will be used to select the states in Nigeria where the project from the WB will be implemented focusing on three key components:

- Desertification Control and Landscape Management
- Community Resilience
- Institutional Strengthening.

## 1.2 Objectives

The present ESA EO Clinic is intended to assist the WB in selecting the most vulnerable states in Nigeria affected by desertification due to the combined effects of climate change and anthropogenic activities, aiming at increasing their agro-climatic resilience. Based on NDVI measurements for the past ~40 years (1982 - 2020) retrieved by four types of satellite data (AVHRR, MODIS, Landsat and Sentinel-2) considering coarse to high spatial resolution, GeoVille has derived trends of land degradation and desertification for the whole country, the states, and different watersheds. Furthermore, GeoVille has scrutinized the ERA-5 re-analysis data to assess trends in temperature and precipitation for the same periods and regions/watersheds to perform a statistical analysis together with the NDVI time series. All produced datasets have been accompanied with confidence intervals to ensure complete transparency and interpretability. On top of that, GeoVille has also produced outreach material and records for capacity building for key stakeholders in Nigeria.



## 2 PROPOSED WORK LOGIC FOR EO-BASED SOLUTIONS

Satellite time-series data of a variety of different sensors (AVHRR, MODIS, Landsat and Sentinel-2) have been analysed for the whole country, including a 25km buffer zone outside the country borders. The assessment is based on NDVI time-series analysis as this is a vegetation-sensitive index that can be derived from all sensors. NDVI measurements for each image and sensor have been calibrated to map the vegetation coverage for each pixel. As an indicator of the vegetation health, yearly time series have been accumulated by integration of the vegetation cover phenology (NDVI vegetation productivity). From this yearly data, linear trends over time can already indicate vegetation loss/gain.

To minimize the influence of climatic variations (e.g., total precipitation), ERA5 reanalysis data was included into the assessment. From this, a climatologically corrected trend analysis was performed, which is used to derive the vegetation development without the influence of yearly climatic deviations.

Both, the uncorrected and the corrected trends were then analysed on an aggregated level, based on spatial polygons for administrative areas and water basins.

### 2.1 Data

Within this project we made use of four different type of satellite data. For the long-term analysis, we relied on the Advanced Very High-Resolution Radiometer (AVHRR) sensor (late seventies) and the Landsat satellite program dating back until the 70ies. The AVHRR provides four- to six-band multispectral data from the NOAA polar-orbiting satellite series. There is fairly continuous global coverage since June 1979, with morning and afternoon acquisitions available. The resolution is 1.1 kilometre at nadir, but the sensor suffered from quality issues and was severely affected by a sensor drift which is a serious drawback for cross-calibration between the various satellite missions. Another long-term earth observation satellite mission is the Landsat mission. It started also in the early 70ies and resulted in 9 satellite missions. In this study we relied a) on Landsat 5 which was launched in 1985 and operated until the end of 2011, 20 years longer than its designated lifetime. Unfortunately, it turned out during production that the coverage with only a few scenes per year provided by Landsat 5 was insufficient for a reliable analysis in the years before 2000 (Figure 1).

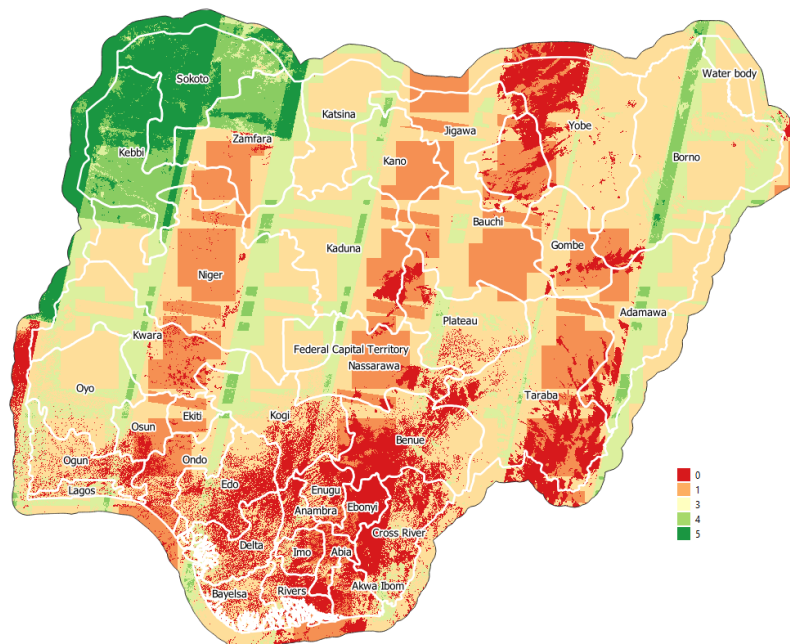


*Figure 1: Landsat 5 number of valid observations in the timeframe between 1995 and 2000: A maximum number of 5 Observations in 5 Years is not enough to estimate the yearly NDVI vegetation productivity. Some areas in the South have no observations at all.*

Additionally, we scrutinized b) Landsat 7 data which was launched in 1999 with the new Enhanced Thematic Mapper Plus (ETM+) sensor that included a 15 m resolution panchromatic band. In May 2003, the scan line corrector of the ETM+ sensor failed and caused striped data gaps. Finally, we made use of c) Landsat 8's Operational Land Imager (OLI) data which improves on past Landsat sensors by providing a 12-bit quantisation of data allowing for a better discrimination of otherwise saturated pixels and improved spectral discrimination of landcover.

For the short-term analysis, we made use of MODIS and Sentinel-2 data. The MODIS instrument is operating on both the Terra and Aqua spacecraft. It has a viewing swath width of 2,330 km and views the entire surface of the Earth every one to two days. Its detectors measure 36 spectral bands between 0.405 and 14.385  $\mu\text{m}$ , and it acquires data at three spatial resolutions -- 250m, 500m, and 1,000m. The last satellite mission which we used to monitor desertification was the Sentinel-2 mission from ESA. Sentinel-2 covers all continental land surfaces (including inland waters) between latitudes 56° south and 84° north. Sentinel-2 carries an optical multispectral instrument (MSI) payload that samples 13 spectral bands with three spatial resolutions: four bands at 10 m, six bands at 20 m and three bands at 60 m spatial resolution.

For an analysis of climatologically independent trends (residual trend analysis) we used the ERA5 land dataset (1979 onwards). ERA5 land is a climate reanalyses product, which combines past observations (as it has evolved during recent decades) with models to generate consistent time series of multiple climate variables on 3D grids at sub-daily intervals. ERA5 land provides hourly gridded estimates for a large number of atmospheric (in our case temperature, total precipitation and radiation), ocean-wave and land-surface quantities.

**Table 1:** Overview of all satellite- and climatological data and its download sources used within this project.

<b>Dataset</b>	<b>Primary download source</b>	<b>Secondary download source</b>
<b>Landsat 5, 7, 8</b>	USGS Earth Explorer <a href="https://earthexplorer.usgs.gov/">https://earthexplorer.usgs.gov/</a>	Amazon Web Services (AWS, Landsat 8 only)
<b>Sentinel - 2</b>	EODC data collection <a href="https://eodc.eu/data/">https://eodc.eu/data/</a>	Amazon Web Services
<b>MODIS, AVHRR</b>	USGS Earth Explorer <a href="https://earthexplorer.usgs.gov/">https://earthexplorer.usgs.gov/</a>	N/A
<b>ERA5 land</b>	ECMWF <a href="https://www.ecmwf.int/">https://www.ecmwf.int/</a> Copernicus Climate Data Store	N/A

**Table 2:** Tabular overview of the investigated time periods and its satellite sources used for the assessment of desertification trends in Nigeria.

<b>Time Period</b>	<b>Nominal resolution</b>	<b>Sensor(s) and datasets</b>	<b>Corrected for climatic variables</b>
<b>1982 - 2020</b>	1000m	AVHRR	YES
<b>1985 - 2020</b>	30m	LANDSAT 5,7,8	YES
<b>2000 - 2020</b>	500m	MODIS	YES
<b>2016 - 2020</b>	10m	SENTINEL-2	LIMITED <sup>1</sup>

<sup>1</sup> Correction has been applied to Sentinel-2 data as well. However, due to the limited time-series of only a few years, the reconstruction and elimination of climatological effects from the data is less accurate.

## 2.2 Methodology

### Terminology

In this context, the term “vegetation productivity” refers to a certain degree of vegetation coverage over one year. For example, a pixel with value 0.5 can be fully covered by vegetation over 6 months or can show 50% coverage throughout the whole year. The full term NDVI vegetation productivity shall indicate that the vegetation coverage for each observation has been retrieved by mapping the coverage to measured NDVI values, as described above.

### Sensor calibration and reliability

During the vegetation and desertification development assessment in Nigeria, a particular focus has been given to the inclusion of multiple sensor (AVHRR, MODIS, Landsat 5,7,8 and Sentinel 2) data. The main factor of comparability between those sensors is the calibration of the retrieved NDVI data to the vegetation coverage of a specific pixel. Since every sensor has slightly different center wavelengths and bandwidths (see table 3 below) and different algorithms used for reflectance calibration, a supervised approach with manual sample polygons has been chosen.

**Table 3:** Tabular overview wavelengths and bandwidths for the different satellite data

	<i>Central wavelength (nm)</i>					
	<i>AVHRR<sup>1</sup></i>	<i>MODIS<sup>2</sup></i>	<i>Landsat 5<sup>1</sup></i>	<i>Landsat 7<sup>1</sup></i>	<i>Landsat 8<sup>1</sup></i>	<i>Sentinel-2<sup>3</sup></i>
<b>Red (VIS)</b>	580 – 680	620–670	630 – 690	630 – 690	640 – 670	664.6 ± 31
<b>NIR</b>	725 - 1100	841–876	760 - 900	770 – 900	850 – 880	832.8 ± 106

<sup>1</sup> Source: usgs.gov

<sup>2</sup> Source: modis.gsfc.nasa.gov

<sup>3</sup> Source: sentinels.copernicus.eu

As a model curve between measured NDVI and vegetation coverage, a sigmoid function has been chosen instead of an often-used linear relationship (see figure 2 below and GPG, as well as references therein). This allows for a direct mapping of arbitrary input values (in this case the NDVI of each pixel) to values between 0 and 1, with the possibility to introduce a measure of uncertainty. Furthermore, this approach allows for calibration of different sensors, including confidence intervals for the calibration coefficients.

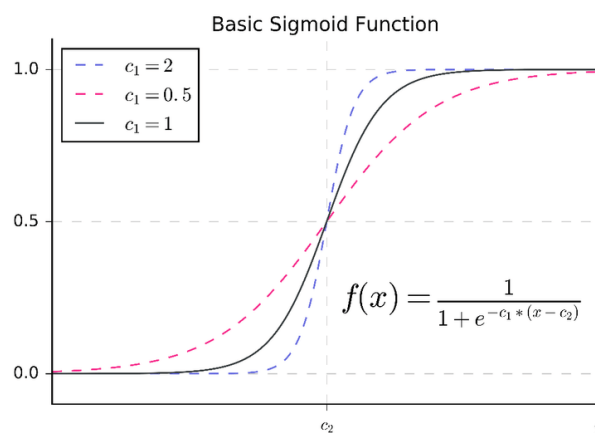


*Figure 2: Parameterized sigmoid function: The parameters c1 and c2 control the position (c2) and smoothness of the curve (c1). C2 is comparable to a classical threshold value which switches between 0 and 1 whereas c1 controls the zone of uncertainty, i.e. increasing values of c1 will lead to a harder transition (smooth transition: red dashed line, harder transition: blue dashed line).*



To achieve a good calibration over the whole country, areas that either show complete vegetation coverage (southern region) or no vegetation at all (northern territory) have been selected manually, and for each pixel and sensor, the corresponding maximum NDVI was extracted.

Figure 3 below shows the selected polygons that have been used for sensor calibration. Depending on the cloud coverage and data quality across all sensors, spots have been chosen that allowed for a clear estimation of the vegetation coverage within the polygon area. For this reason, some spots lie outside the country to include the whole spectrum of vegetation responses. The calibration was then performed on the same polygons for all sensors using logistic regression.

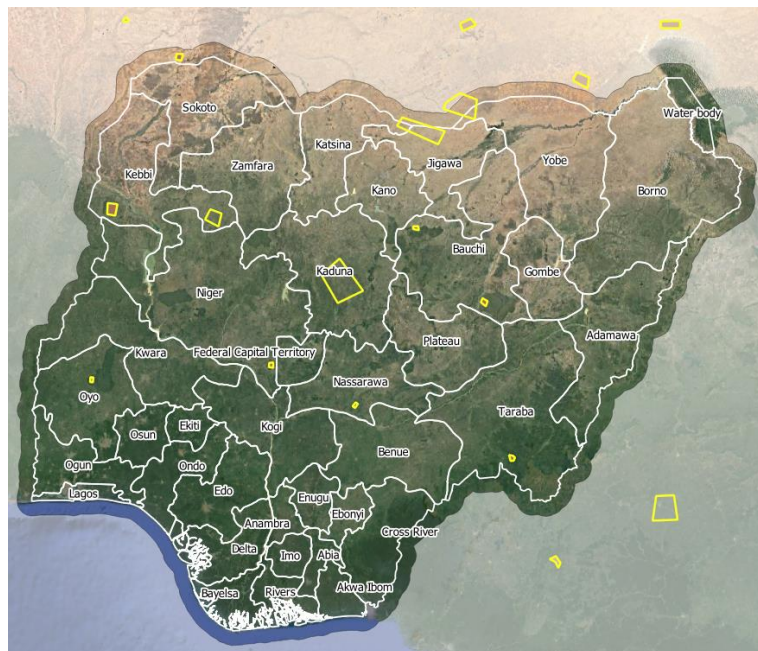


Figure 3: Polygons (yellow outline) used for the sensor calibration for all satellite data.

The following table 4 shows, after the successful calibration operations, the retrieved calibration coefficients for each sensor. A comparison between the errors of the  $C_2$  coefficient with its corresponding mean value reveals that the transition zone (i.e. the classical threshold value) can be calibrated very accurately. However, a rather large sensor-specific transition zone (given by the parameter  $C_1$ ) corresponds to areas only partly covered by vegetation. Depending on the type and quality of the sensor data, the mapping of these intermediate values is accompanied by a certain level of uncertainty, meaning that in these areas, the NDVI can only be mapped approximately to a certain vegetation coverage value.

**Table 4:** Retrieved calibration coefficients for each sensor.

<b>SENSOR</b>	<b>C1</b>	<b>C1 ERROR</b>	<b>C2</b>	<b>C2 ERROR</b>
<b>S2</b>	57.3	0.3	0.2527	1E-4
<b>MODIS</b>	101.8	0.5	0.39480	6E-5
<b>AVHRR</b>	86.9	0.4	0.24293	6E-5
<b>LS5</b>	85.4	0.4	0.18525	8E-5
<b>LS7</b>	105.0	0.5	0.26902	6E-5
<b>LS8</b>	52.2	0.2	0.2989	1E-4

## NDVI Vegetation productivity time series calculation

After calibration and vegetation coverage mapping for each sensor and observation, the calculation of the yearly NDVI vegetation productivity is carried out by the following steps:

### 1. Calculation of the NDVI

The NDVI is calculated for each single scene and the sensor dependent calibration curve is applied. This gives an estimation of the vegetation coverage for each image.

### 2. Vegetation modelling and integration

Vegetation curves are modelled with a 3<sup>rd</sup> degree fourier series (see ,e.g., Jakubauskas et al., 2001, and Jönsson and Eklundh, 2004 for similar approaches). From this model curve, the mean squared deviation of the time series is calculated.

The NDVI vegetation productivity P is then calculated through integration by using the trapezoidal rule:

$$P = \sum_{i=1}^{N-1} \frac{f_{i+1} + f_i}{2} (t_{i+1} - t_i)$$

### 3. Error propagation

Errors for the NDVI productivity values are retrieved by gaussian error propagation:

$$\Delta f = \sqrt{\left(\frac{\partial f}{\partial x} \Delta x\right)^2 + \left(\frac{\partial f}{\partial x_0} \Delta x_0\right)^2 + \left(\frac{\partial f}{\partial \alpha} \Delta \alpha\right)^2}$$

and

$$\Delta P = \Delta t \cdot \sqrt{\frac{\Delta f_1^2 + \Delta f_N^2}{4} + \sum_{i=2}^{N-1} \Delta f_i^2}$$

With  $\Delta x$  being the mean squared deviation from the model curve and  $\Delta x_0$  and  $\Delta \alpha$  being the errors from te calibration coefficients.

## 3 DELIVERED EO-BASED PRODUCTS AND SERVICES

### 3.1 Raster maps

During production, the whole archives of available data for the listed sensor has been explored and evaluated for usability and quality.

The originally proposed timespan for the low-resolution time-series of AVHRR from 1982 onwards could be extended to also include 1981 through partly extrapolated data. All the maps of this sensor have been processed with a resolution of 5 km as opposed to 1 km since the used dataset (NOAA CDR AVHRR: Surface Reflectance, Version 5) only offers a resolution of 0.05° (see Vermote, E. & NOAA CDR Program, 2018). This dataset was chosen because it offers, as stated in the reference, “*more accurate approaches for BRDF correction (Bidirectional Reflectance Distribution Function), calibration, compositing, and QA. Version 5 also corrects the data for known errors in time, latitude, and longitude variables, as well as improves the global and variable attribute definitions*”.

All maps including Landsat/Sentinel-2 data have been produced in 250m resolution as our investigations have shown that the statistical trend analysis is not negatively affected by the aggregation to a coarser resolution (See figure 4 below).

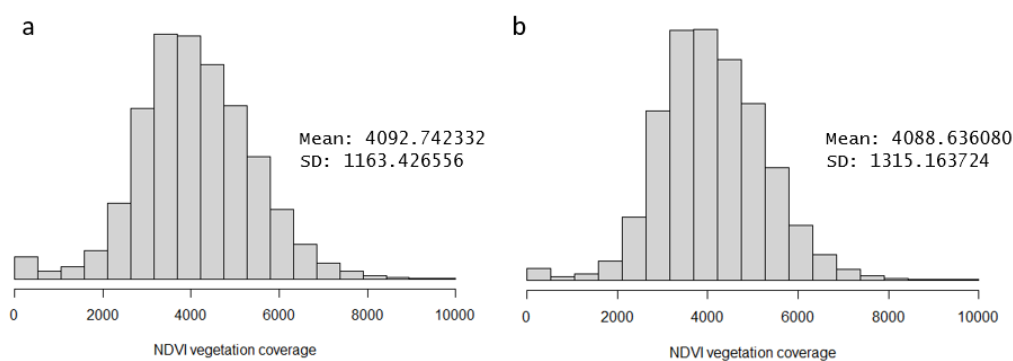


Figure 4: Comparison of the Landsat based NDVI vegetation productivity histograms in the district Niger for the production year 2015: 30m high resolution aggregates (a) show virtually the same distribution as the lower resolution version (b, 250m).

On the other hand, this aggregation allows for a reduction of the errors in single pixel measurements through averaging and simplifies a direct comparison with the MODIS data.

In addition to the proposed raster maps, NDVI vegetation productivity change maps for each sensor will be included in the data delivery. These maps shall give an insight into the spatial distribution of the vegetation development on an annual basis.

Also, the data delivery includes binary desert classifications derived from the productivity status maps with a threshold below 10% (almost no vegetation) and a threshold below 30% (sparsely vegetated areas included). A description of how to derive binary classifications and probabilities using different thresholds is included in this document.

In addition to the raster maps, the MODIS based NDVI vegetation productivity has been compiled into a video which gives a visual impression on the vegetation development and desertification.

The following table 5 lists all the raster products that have been produced.

**Table 5:** Product overview of all raster maps produced within this project.

Product	Sensor	Time frame	Resolution
Annual productivity time series, including confidence layers	AVHRR	1981 – 2021	5000m
	MODIS	2000 – 2021	250m
	Landsat 5, 7, 8	2000 - 2021	250m
	Sentinel-2	2015 – 2021	250m
Desert, binary classification map, including confidence layers	AVHRR	1981 – 2021	5000m
	MODIS	2000 – 2021	250m
	Landsat 5, 7, 8	2000 - 2021	250m
	Sentinel-2	2015 – 2021	250m
Sparse vegetation, binary classification map, including confidence layers	AVHRR	1981 – 2021	5000m
	MODIS	2000 – 2021	250m
	Landsat 5, 7, 8	2000 - 2021	250m
	Sentinel-2	2015 – 2021	250m
Productivity change maps, including confidence layers	AVHRR	1981 – 2021	5000m
	MODIS	2000 – 2021	250m
	Landsat 5, 7, 8	2000 - 2021	250m
	Sentinel-2	2015 – 2021	250m

### 3.2 Vector maps

Trend analysis was performed on a district level and on water basin polygons. The trend values are stored as data frames and included into the vector products. All polygons include values for the NDVI vegetation productivity trends (uncorrected) as well as for the extracted residual trends (corrected for climatic influences).

The following sensors and timeframes (table 6) have been processed:

**Table 6:** Product overview of all vector maps produced within this project.

Product	Sensor	Time frame	Base resolution
District level analysis	AVHRR	1985 – 2018	5000m
	AVHRR	2000 – 2017	5000m
	Landsat 5, 7, 8	2000 – 2020	250m
	MODIS	2000 – 2017	250m
	MODIS	2000 – 2020	250m

	Sentinel - 2	2016 – 2020	250m
Water basin analysis	MODIS	2000 - 2020	250m

### 3.2.1 Specifications

All products are delivered in WGS84 (EPSG:4326) projection and cover the same extent, which spans over the whole national territory with an additional buffer of 25km.

All raster maps are delivered as LZW compressed tiff files with the resolution indicated above.

Vector maps are delivered as ESRI Shapefiles.

### 3.2.2 Usage, Limitations and Constraints

NDVI vegetation productivity maps can be used as common bases for all derived spatial and temporal analyses. They serve as a vegetation status product and include confidence intervals on a pixel level.

The change maps included in the delivery are an example of such a derived product, giving estimates for both the productivity change and the propagated confidence level on an annual basis. A limitation of such yearly change maps is the lower confidence due to error aggregation (for the change, the uncertainties of both years accumulate according to gaussian error propagation). This means, that only an indication of the vegetation development can be given on a pixel level.

Binary maps are also derived from the NDVI vegetation productivity and are includes as two different threshold levels. The first one (threshold below 10%) is mostly depicting areas with almost no vegetation, i.e. deserts and shall focus on pure desert areas. The second one also includes areas of sparse vegetation (threshold below 30%) and also focuses on the delineation and development of areas with low vegetation cover, i.e. the transition zones between desert and vegetated landscapes.

### 3.2.3 NDVI annual vegetation productivity

Raster maps are available for all sensors and all possible years. The maps give a per-pixel, uncorrected value for the RAW productivity together with confidence intervals.

An example of the MODIS based calculation as well as a qualitative sensor comparison is shown in the Figure 5 below.

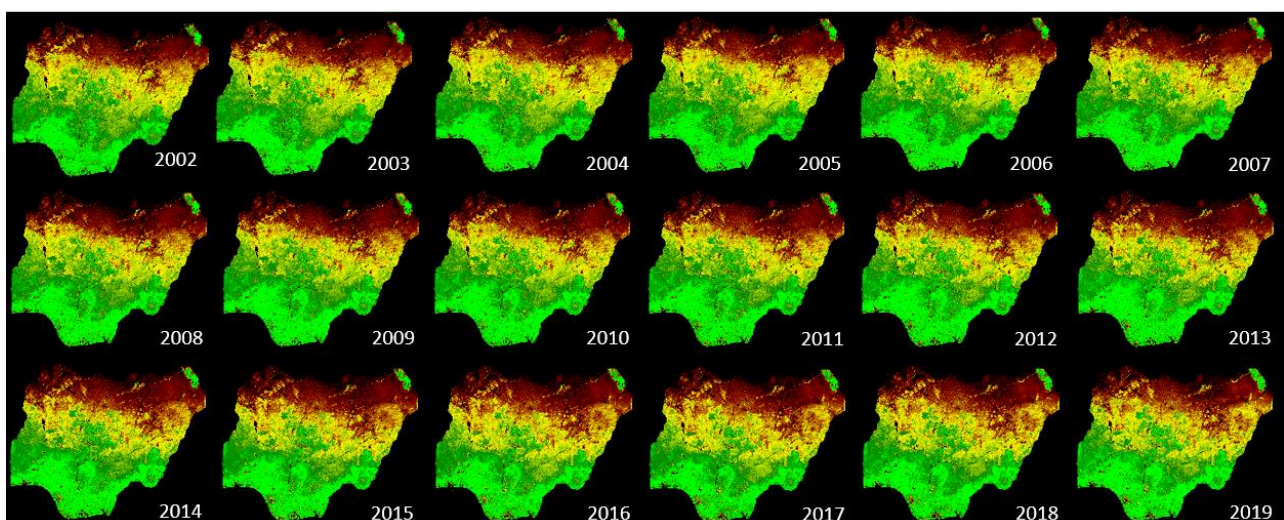


*Figure 5: MODIS based raw NDVI vegetation productivity values from 2002 onwards.*



A special focus of the production has been given to the calibration and harmonization of the different sensors to retrieve a comparable result across the different data sources. The Images below (Figure 6) shall give an impression of the achieved results and compare values for the production year 2018. Visually, only small differences can be spotted, for example in the south (red circles) where the two high resolution sensors indicate less vegetation coverage than AVHRR and MODIS. Differences are mostly seen in the transition zones between vegetated and unvegetated areas. This is in line with the uncertainty of the calibration curves which show the highest error propagation around the 50% mark of the vegetation mapping.

Numerical analysis has shown that the trends derived across different sensors are very sensitive to small deviation and can only deliver an indication on the trend development. It is therefore advised to use these maps as proxies for further detailed analysis based on high resolution data and possibly also backed by ground truth data.

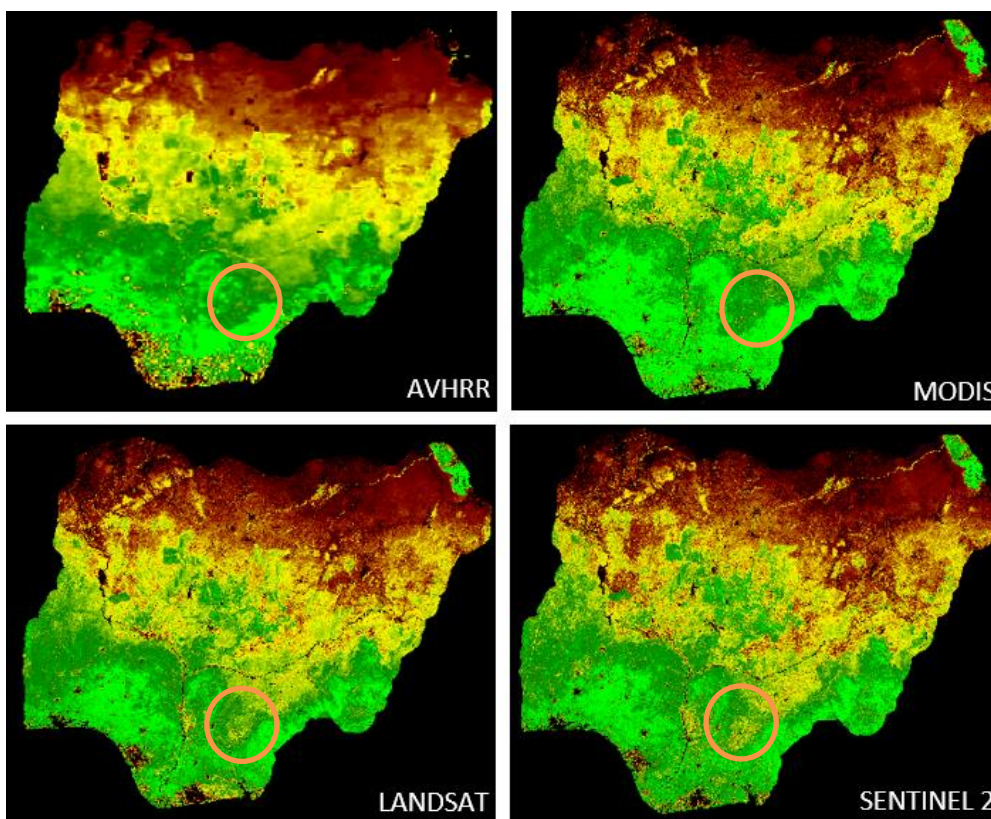


Figure 6: Sensor comparison for the year 2018. Clearly visible is that the high-resolution sensors depict less vegetation coverage than the rough ones (red circles).

### 3.2.4 Yearly productivity change and binary desert map

For the calculation of the change of two consecutive years, the difference of two consecutive images is calculated on a pixel level. Error propagates according to

$$\Delta x_{change} = \sqrt{\Delta x_{year1}^2 + \Delta x_{year2}^2}$$

An example of the productivity change from 2018 to 2019 is given in Figure 7.

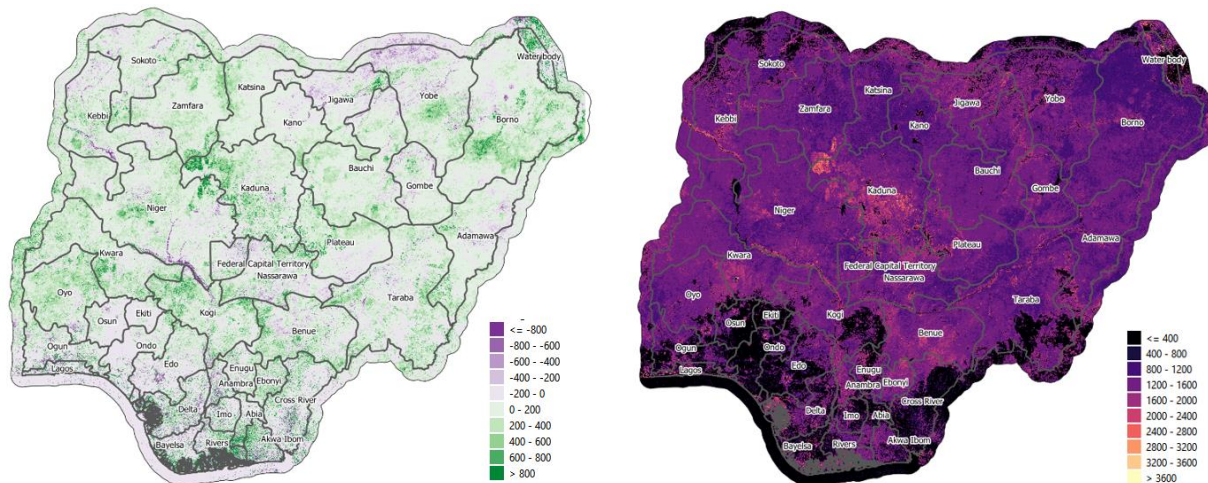


Figure 7: MODIS Productivity change (left) and change confidence (right), Year 2018/19. Values have been scaled by a factor of 10000, i.e., 10000 equals 1%.

This analysis shows that the change values for 1 year are usually below 8% (value 800) with a mean confidence of about 10%. Exact values of change and change confidence are given on a pixel level and can be extracted for each sensor and year from the delivered products. Overall, in many cases no clear conclusion on the vegetation development can be made on a pixel level and on a yearly basis, i.e., the confidence interval often spreads across slight gain and loss. These uncertainties are a result of the natural uncertainty of the vegetation coverage mapping and the uncertainties coming from the sensor itself, e.g., sensor noise, atmospheric interference etc.

### 3.2.5 Binary vegetation maps

This product contains binary maps of areas that fall below a certain threshold of vegetation coverage. Included are maps for a threshold below 10% (desert areas or water bodies) and 30% (including also sparsely vegetated areas).

Along with the binary map, also the probability is given, which is retrieved by integration of the normal distribution of each point, i.e.:

$$\frac{1}{2} \cdot \left[ 1 + \operatorname{erf} \left( \frac{th - P}{\Delta P \sqrt{2}} \right) \right]$$

Where  $th$  denotes the binary threshold (i.e., 10% or 30%),  $P$  the NDVI vegetation productivity value and  $\Delta P$  the confidence for each pixel. Erf denotes the Gaussian error function.

Below, in Figure 8 an example of a 30% desert map is shown.

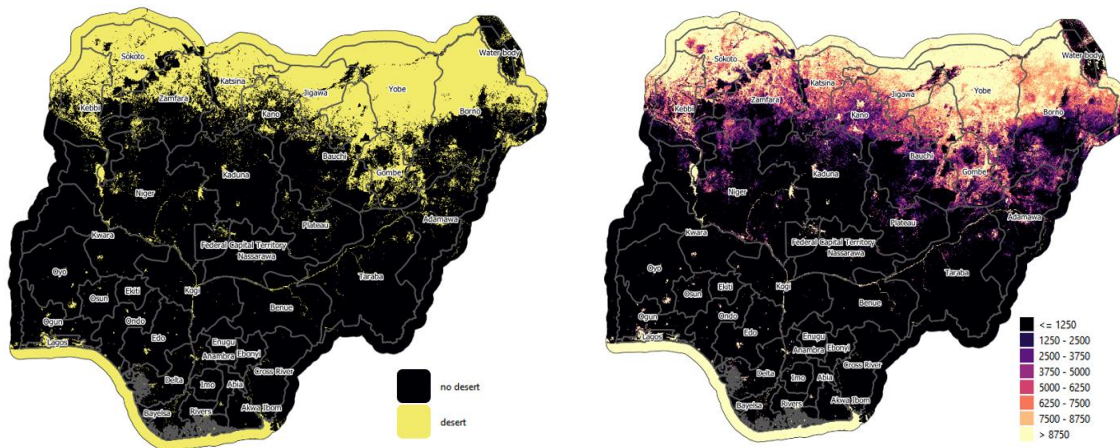


Figure 8: Binary classification (left) and classification confidence (right, values scaled by 10000), Year 2018.

### 3.2.6 Aggregated Analysis and residual trend

#### Residual trend

The NDVI productivity is calculated only based on the satellite measurement regardless of climatic influences such as precipitation or radiation. However, depending on the type of analysis, it might be necessary to correct for these influences, e.g., a vegetated area might show less coverage in a year with lower total precipitation, resulting in a lower NDVI productivity value. However, in this case, no actual change of the landcover has taken place.

One possibility to correct for these influences is a residual trend analysis (see, e.g., GPG). This method assumes that climatic variables can at least partly describe fluctuations of productivity. To correct for these influences, a model between measured NDVI productivity and climatic values is calculated, and the effect of the model is subtracted from the observed values. Subsequently, only the trend on the remaining deviations, i.e., the trend on the residual values is analysed.

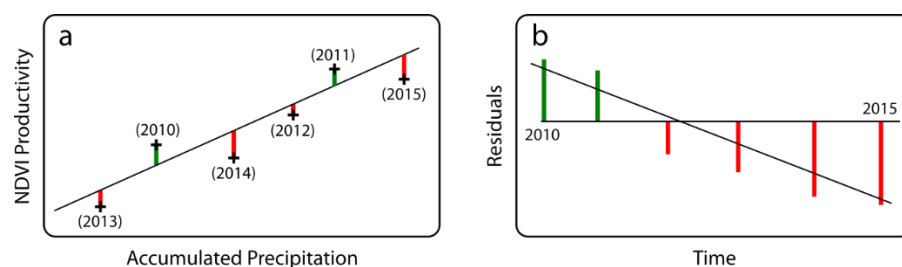
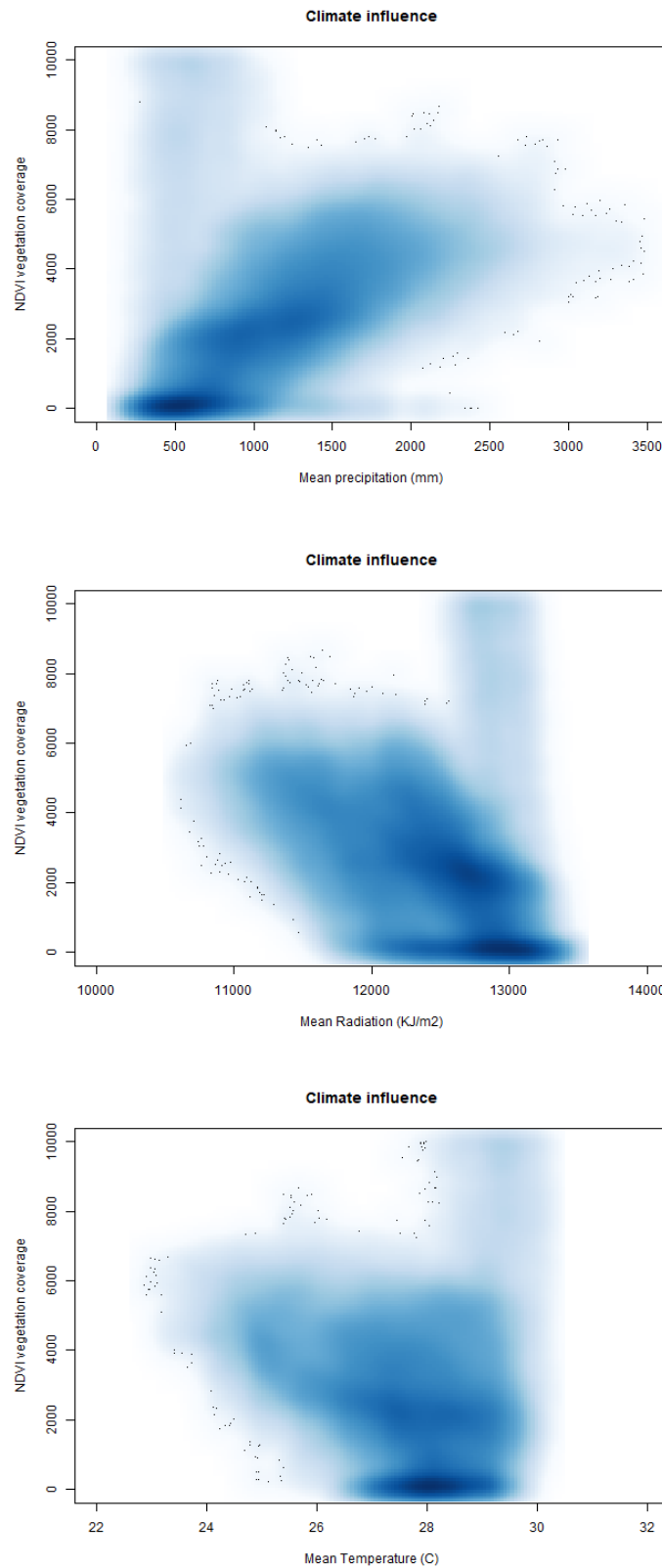


Figure 9: Illustration of the residual trend method. a: Precipitation is fitted against NDVI productivity and the residuals are calculated. b: The residuals are analysed for a trend in time.

In this case, the climatic variables precipitation, insolation (radiation) and surface temperature have been extracted from the ERA5 land reanalysis data for each observation year. As a model, a **multilinear regression** has been performed. Below, in Figure 10 an example of the relationship between these variables and the observed NDVI productivity is given.



*Figure 10: Influence of precipitation, insolation (radiation), and surface temperature on the NDVI productivity. Shown are all pixel values from the MODIS observation above 10 degrees latitude.*



This observation shows a slight relationship from precipitation and radiation, but no visible dependence on the temperature values. This is in line with the observation from Hashimoto et al. (2019) which indicates that the vegetation in Nigeria is mostly dependent on these two variables, as can be seen in the figure below.

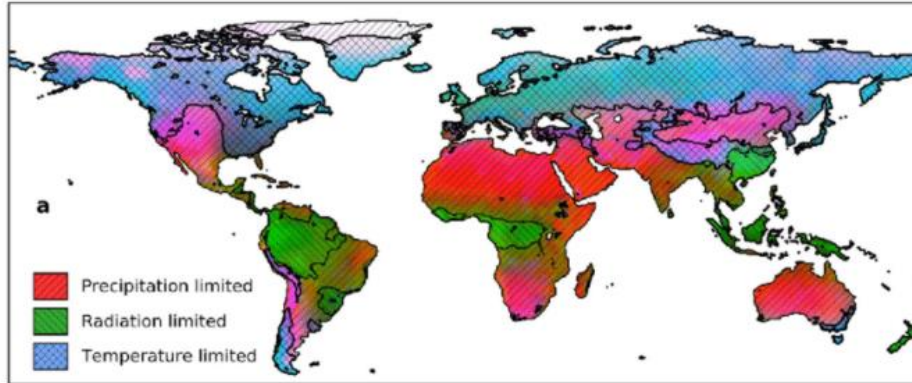


*Figure 11: Main limiting factors of vegetation development according to Hashimoto et al. (2019).*

### **Statistical analysis**

For a statistical analysis based on spatial polygons (such as administrative districts), all NDVI productivity values of a certain polygon have been extracted and analyzed for a linear trend in time. This analysis has been performed on both the uncorrected NDVI productivity values and on the residuals of the climatic modelling.



## 4 EVALUATION AND FOLLOW-UP ACTIVITIES

### 4.1 Key findings

#### Trend analysis (districts & hydro basins)

The following images show trend analyses of district as well as water basin levels. As explained above, the analysis shall be focused on MODIS time series as this is considered the most reliable sensor. Trend analysis has been performed between 2000 and 2021.

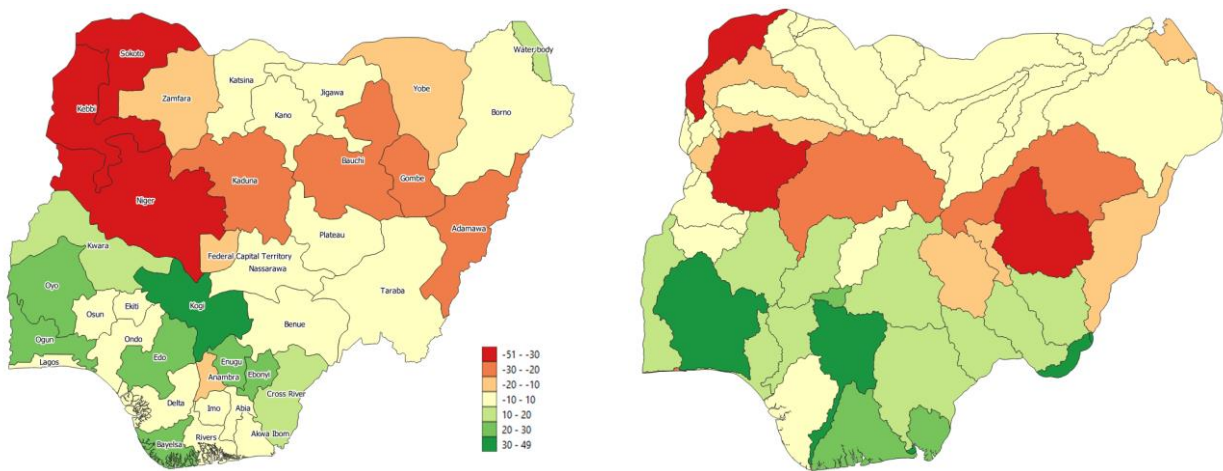


Figure 12: MODIS based residual trend analysis (climate-related vegetation response eliminated to the best possible extent, i.e., most likely anthropogenic vegetation response), per district (left) and per basin (right)

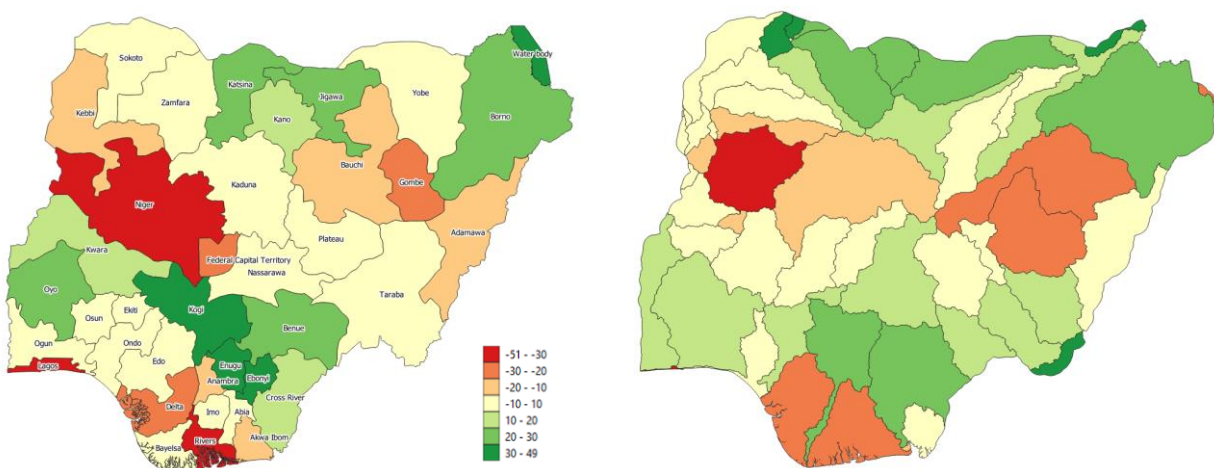


Figure 13: MODIS based uncorrected NDVI vegetation productivity trend analysis (including all factors, i.e., climate and human activities), per district (left) and per basin (right).

## AVHRR

Even though AVHRR is considered less reliable due to orbital drift effects and overall noisy and observations of lower quality, it is the only single sensor observation data that covers the time span from the above presented MODIS trends. Below a qualitative comparison on district level is given. The colour scheme shall be seen as qualitative comparison only, as the AVHRR data is not reliable over time and shows a negative trend in most districts due to inconsistent time series.

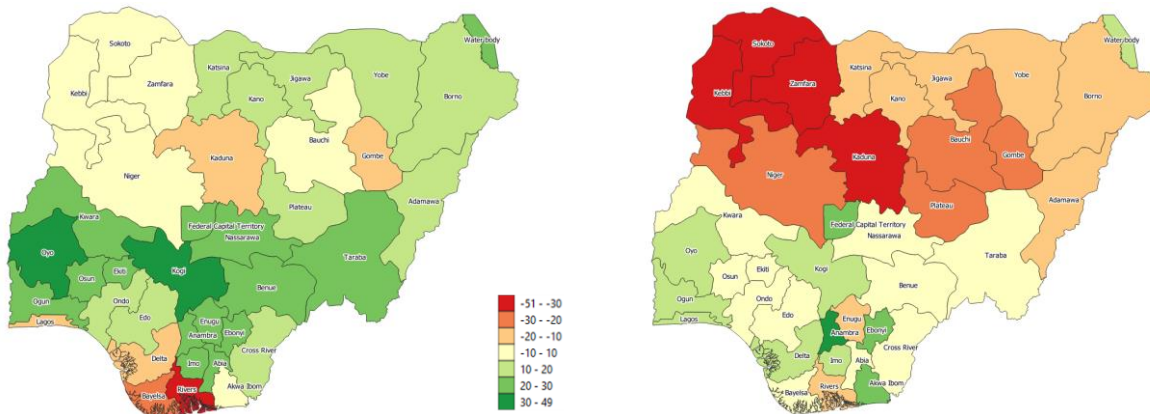


Figure 14: Left: AVHRR based residual trend (climate-related vegetation response eliminated to the best possible extent, i.e., most likely anthropogenic vegetation response), right: AVHRR based raw NDVI vegetation productivity trend (including all factors, i.e., climate and human activities)

## Analysis

From the MODIS residual trend analysis, it can be seen that the north-west districts **Sokoto**, **Kebbi** and **Niger** show the strongest and most consistent negative trend. This indicates a vegetation loss in these districts. Absolute values for these districts are a loss of 0.3% (Sokoto), 0.5% (Kebbi) and 0.3% (Niger) in the time between 2000 and 2020. Below, plots are shown (Figure 15) to give a more detailed look onto these districts.

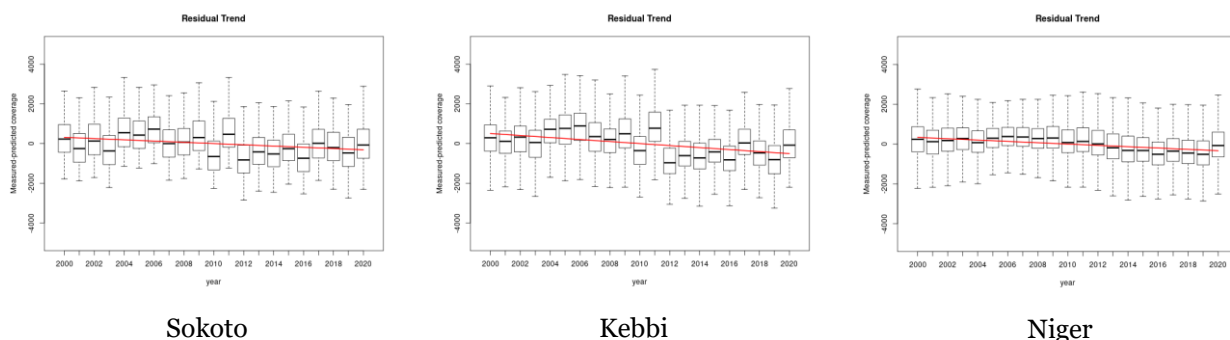


Figure 15: Statistical trends and its uncertainties for the most affected states in Nigeria.

Even though a clear negative overall trend is visible, it has to be mentioned that the spread of the observations is relatively high in each year, with a relatively clear increase in the last observation year which should be further analysed with the help of local studies and in-situ data. **Sokoto and Kebbi** show an additional unusual high value in 2011 which could indicate a climatic event, e.g., unusually increased precipitation which could not be fully eliminated with multilinear correction approach.

The comparison with AVHRR, even though considered less reliable, also gives an indication that the north-western part of the country shows the highest vegetation degradation.

No strong positive trends could be seen in the analysis for the areas close to the desert transition zone. Stagnation or a very slight increase of vegetation can be observed in the districts **Katsina, Kano, Jigawa**. In these regions, the raw NDVI vegetation productivity trends suggest a positive development, however, the climatic corrected data is pointing more towards the interpretation that these effects are caused by the positive climatic influence.

As an overview, all of the trend values (corrected and uncorrected) that have been retrieved by the MODIS analysis are summarized in table 7 below.

**Table 7:** MODIS based NDVI vegetation productivity trends and residual trends. Negative values indicate a loss of vegetation.

<b>District</b>	<b>NDVI productivity trend</b>		<b>Residual trend</b>	
<b>Abia</b>	-0,007	± 0,027	-0,022	± 0,026
<b>Adamawa</b>	-0,179	± 0,016	-0,244	± 0,010
<b>Akwa Ibom</b>	-0,136	± 0,019	0,081	± 0,018
<b>Anambra</b>	-0,122	± 0,043	-0,177	± 0,037
<b>Bauchi</b>	-0,137	± 0,013	-0,251	± 0,008
<b>Bayelsa</b>	-0,094	± 0,028	0,227	± 0,026
<b>Benue</b>	0,229	± 0,011	0,088	± 0,008
<b>Borno</b>	0,228	± 0,008	0,071	± 0,005
<b>Cross River</b>	0,103	± 0,012	0,185	± 0,011
<b>Delta</b>	-0,296	± 0,023	0,020	± 0,022
<b>Ebonyi</b>	0,384	± 0,020	0,266	± 0,018
<b>Edo</b>	0,068	± 0,013	0,201	± 0,011
<b>Ekiti</b>	0,062	± 0,014	0,099	± 0,013
<b>Enugu</b>	0,303	± 0,020	0,239	± 0,020
<b>Federal Capital Territory</b>	-0,210	± 0,026	-0,125	± 0,025
<b>Gombe</b>	-0,240	± 0,017	-0,255	± 0,015
<b>Imo</b>	-0,022	± 0,018	-0,030	± 0,018
<b>Jigawa</b>	0,253	± 0,013	-0,021	± 0,011
<b>Kaduna</b>	-0,065	± 0,014	-0,216	± 0,010
<b>Kano</b>	0,126	± 0,013	0,017	± 0,010
<b>Katsina</b>	0,248	± 0,013	-0,014	± 0,007
<b>Kebbi</b>	-0,167	± 0,016	-0,508	± 0,012
<b>Kogi</b>	0,399	± 0,013	0,490	± 0,011
<b>Kwara</b>	0,138	± 0,010	0,110	± 0,008
<b>Lagos</b>	-0,516	± 0,097	-0,055	± 0,089
<b>Nassarawa</b>	-0,081	± 0,012	-0,097	± 0,011
<b>Niger</b>	-0,319	± 0,008	-0,334	± 0,008

<b>Ogun</b>	0,065	± 0,017	0,204	± 0,015
<b>Ondo</b>	0,037	± 0,013	0,089	± 0,013
<b>Osun</b>	0,067	± 0,016	0,091	± 0,015
<b>Oyo</b>	0,257	± 0,011	0,277	± 0,011
<b>Plateau</b>	-0,007	± 0,013	-0,092	± 0,011
<b>Rivers</b>	-0,579	± 0,041	0,073	± 0,039
<b>Sokoto</b>	0,076	± 0,014	-0,314	± 0,011
<b>Taraba</b>	0,006	± 0,014	-0,015	± 0,009
<b>Water body</b>	0,427	± 0,076	0,104	± 0,074
<b>Yobe</b>	-0,005	± 0,009	-0,162	± 0,007
<b>Zamfara</b>	0,083	± 0,015	-0,193	± 0,010

### Sensor reliability

One of the key findings of this assessment was the possibility for a direct sensor comparison and reliability ranking.

For a long-term analysis, we rank the reliability of the sensors in the following way:

1. **MODIS:** Available since 2000 with a resolution of 250 (NDVI bands). The sensor operated on the Terra and Aqua satellites is very stable in terms of reflectance values with a high observation frequency. For this assessment, this is the only single-sensor study that covers the whole-time range with moderate resolution.
2. **AVHRR:** The sensor offers data since 1982 in coarse resolution. It is by far the sensor with the longest time-range (flown on multiple NOAA satellites). However, data before around 2000 is of lower quality because of stability problems (i.e., orbital drift leading to increasing solar zenith angles and thus a change in the reflectance behaviour of the underlying surface) in the early years of operation (Figure 16). Also, due to the low resolution and less statistics, errors and noise in the pixel data are carried to the aggregated analyses (e.g., trend analysis of a certain area) which makes them less trustworthy. AVHR sensor drift has been already discussed in multiple publications, see for example Kaufmann (2000), Ignatov (2004) or Ji (2017).

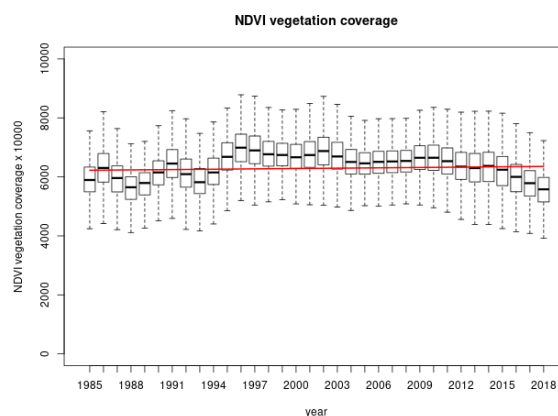


Figure 16: AVHRR based mean vegetation coverage in the district Niger. The data before 1997 shows a higher variability than the data from around 2000 onwards. This behaviour is attributed to sensor drift which lowers the reliability of the long-time analysis.

3. **Sentinel-2:** High resolution of 10m and a high observation frequency in combination with stable operation makes the data retrieved from this sensor very valuable. Unfortunately, the data is only available from mid-2015 onwards and therefore a Sentinel-2 long-term analysis is not possible.
4. **Landsat 5/7/8:** Landsat 5 should in principle be available since 1984. However, not all the data from this time has been archived and the data analysis during the project development has shown that only a few Landsat 5 images are available in the AOI. Therefore, NDVI productivity calculation could only be performed from 2000 onwards using Landsat 7 and Landsat 8 data. On 31 May 2003, the Scan Line Corrector (SLC) in the ETM+ of Landsat 7 instrument failed, resulting in stripe artefacts in each image. Moreover, even though the calibration has been performed separately on each sensor, small differences remain which can introduce a bias in the trend analysis.

## 4.2 Outlook and further studies

The extension of the service to other regions around the Great Green Wall, is in general possible and GeoVille is prepared to initiate such a service. From a methodological point of view, we don't see larger issues by transferring the mapping approaches to other areas, as long as the investigation relies on MODIS data (no calibration issues and constituent over time) and focuses on the time frame from 2000-2020.

If the vegetation trend analysis would like to be extended in time and at a higher spatial resolution, more in depth-analysis are needed. We don't suggest extending the time period by relying on AVHRR data. This is first due its rough resolution and secondly due to cross-calibration issues within the AVHRR data itself. GeoVille rather would suggest extending the analysis towards a higher resolution using Sentinel-2 and Landsat 8 data. Sophisticated methods exist to calibrate the different data together (as already shown in this study), but nevertheless a higher number of in-situ-calibration data would be needed for both, calibration, and validation to receive robust results. If such data are available or can be collected, for example in the form of sample polygons in areas with a known vegetation cover that is constant over the investigation period, also a sensor calibration on a yearly basis would be possible to counter-act remaining differences in the data.

Furthermore, it might be of interest to carry out visual, high-resolution analysis in selected regions to support the findings and observations. For this, a few scenes with a very high resolution could be used to visually estimate the mean vegetation coverage on several sample points which could then be used for validation purposes.

The team is furthermore available to advise on and provide proven solutions aimed at supporting decision making in the context of mitigation actions during the implementation phase.



---

## APPENDIX A: REFERENCES

GPG: Good Practice Guidance SDG Indicator 15.3.1, [https://www.unccd.int/sites/default/files/relevant-links/2021-03/Indicator\\_15.3.1\\_GPG\\_v2\\_29Mar\\_Advanced-version.pdf](https://www.unccd.int/sites/default/files/relevant-links/2021-03/Indicator_15.3.1_GPG_v2_29Mar_Advanced-version.pdf), accessed 28.10.2021.

Jakubauskas, M. E., Kastens, D., & Jude (2001). Harmonic Analysis of Time-Series AVHRR NDVI Data. *Photogrammetric Engineering and Remote Sensing*, 67(4), 461–470.

Jönsson, P., & Eklundh, L. (2004). TIMESAT—a program for analyzing time-series of satellite sensor data. *Computers & Geosciences*, 30(8), 833–845.

Ji, L., & Brown, J. F. (2017). Effect of NOAA satellite orbital drift on AVHRR-derived phenological metrics. *International journal of applied earth observation and geoinformation*, 62, 215–223.

Kaufmann, R. K., Zhou, L., Knyazikhin, Y., Shabanov, V., Myneni, R. B., & Tucker, C. J. (2000). Effect of orbital drift and sensor changes on the time series of AVHRR vegetation index data. *IEEE Transactions on Geoscience and Remote Sensing*, 38(6), 2584–2597.

Ignatov, A., Laszlo, I., Harrod, E. D., Kidwell, K. B., & Goodrum, G. P. (2004). Equator crossing times for NOAA, ERS and EOS sun-synchronous satellites. *International Journal of Remote Sensing*, 25(23), 5255–5266.

Hashimoto, H., Wang, W., Melton, F. S., Moreno, A. L., Ganguly, S., Michaelis, A. R., and Nemani, R. R. (2019) High resolution mapping of daily climate variables by aggregating multiple spatial data sets with the random forest algorithm over the conterminous United States. *International Journal of Climatology* 39(6): 2964–2983.

Vermote, E. & NOAA CDR Program. (2018). NOAA Climate Data Record (CDR) of AVHRR Surface Reflectance, Version 5 [Data set]. NOAA National Centers for Environmental Information. <https://doi.org/10.7289/V53776Z4>.